Medium Voltage Converter Inductor Insulation Design Considering Grid Insulation Requirements

Haiguo Li[1*], Pengfei Yao[1], Zihan Gao[1], Fred Wang[1,2]
[1]Min H. Kao Department of Electrical Engineering and Computer Science, the University of Tennessee, Knoxville, TN, USA
[2]Oak Ridge National Laboratory, Oak Ridge, TN, USA
*hli96@vols.utk.edu

2021 IEEE Applied Power Electronics Conference and Exposition (APEC) | 978-1-7281-8949-9/21/$31.00 ©2021 IEEE | DOI: 10.1109/APEC42165.2021.9487031

***Abstract*—Medium voltage SiC devices facilitate direct (without 50/60 Hz transformer) connection of the power electronics converter to the medium voltage grid using simple topology. Compared to the insulation design of medium voltage inductors that have been widely used in the power system, the insulation design of directly connected medium voltage converter filter inductors has more challenges. Although some works has been done discussing that, the grid insulation requirements on converter filter inductors are rarely discussed. This paper introduces the insulation design of a grid-side filter inductor for a 13.8 kV power conditioning system converter. The grid insulation requirements, including the short-duration power frequency overvoltage and the lightning impulse voltage, are considered in the design. To meet the requirements, the layer-to-layer insulation, winding-to-core/ground insulation, the air gap discharge between the winding and the core, as well as the local electrical field have been taken into consideration. Experimental tests are provided to validate the design.**

Keywords—Medium voltage, converter, inductor, insulation, grid insulation requirements

I. INTRODUCTION

With medium voltage (MV) SiC devices, power electronics converters can be directly (without 50/60 Hz transformer) connected to the MV grid with simple topologies [1], while this requires high insulation capability of the converter filter inductor. Although MV low frequency (50/60 Hz) inductors have been widely used in the power system, they are large and heavy because of the high power rating. Besides, these inductors are mostly designed with silicone steel core and only need to consider the fundamental current. However, besides the fundamental current, there are also high switching current ripples flowing through the power electronic converter inductors, which will induce additional winding and core losses. Also, converter filter inductors generally have less current rating, and the inductance is also small (e.g., 0.01 p.u. or even less) because of the high switching frequency of SiC devices [2]. It is essential to design a small inductor to fully utilize the benefits of SiC devices. Then, the insulation design of the converter inductor becomes a big challenge because the insulation requirements are not changed (same voltage level), but the smaller size means less room for insulation.

There have been some works discussing the MV converter inductor and transformer insulation design, and they can be divided into two categories based on their insulation methods.

One method is based on the insulation layers and air gap clearance, and this is more used at low voltage levels. In [3], several inductors are connected in series to reduce the winding voltage drop of each inductor, and Nomex insulation paper and Kapton tape are used between the windings and the core. In [4], a bobbin made of insulation material has been used for the insulation between winding and core, and an air gap clearance was used to do insulation between winding layers.

The other method is based on casting or encapsulation, and this is normally used at higher voltage levels. In [5], the windings are encapsulated in the 3D-printed coil former with silicone, and spacers are used to keep the distance between the coil former and the core. In [6], the winding has been immersed in 1-K impregnating at first and then covered with a semi-conductive tape to get a smooth electrical field, followed by another 2-K vacuum casting. In [7], to achieve the insulation capability, the MV windings are encapsulated with epoxy and then covered by a semiconductive shield connected to the ground. Although different insulation methods have been used, the grid insulation requirements, especially the lightning impulse withstand voltage and the short-duration power frequency withstand voltage, are not discussed in those works.

To meet grid insulation requirements, a much higher insulation voltage, compared to the normal operation voltage, needs to be considered, which will make the insulation design more challenging. The grid insulation requirements are considered in [8], but the large air gap used to avoid partial discharge (PD) increases the overall size significantly.

In this paper, the design of an AC filter inductor for a 13.8 kV cascaded H-bridge (CHB) based grid-connected converter is introduced, considering grid insulation requirements. An inductive shielding on the winding surface is applied, to stress the winding-to-ground potential on the insulation material and avoid the discharge of the air gap between the winding and the core.

The rest of this paper is organized as follows. First, the system configuration and the inductor parameters are introduced in Section II. Then, the inductor insulation design is discussed in Section III. The first version of the inductor has been built and tested in Section IV and Section V. The second version of the inductor has been designed and built in Section VI, based on the test results shown in Section IV and V. Finally, this paper concludes with Section VII.

II. SYSTEM CONFIGURATION AND INDUCTOR BASIC DESIGN RESULTS

As shown in Fig. 1, a power conditioning system (PCS) converter is used to connect an 850V DC to the 13.8 kV AC grid. The PCS converter consists of a DC/DC stage and a DC/AC stage, and this paper mainly focuses on the DC/AC stage so the DC/DC stage will be neglected in the following discussion. The MV DC-links are rated at 6.7 kV, and 10 kV SiC MOSFETs are used, with a switching frequency of 10

kHz. The DC/AC stage has 2 full bridges in series and outputs five-level voltages, so the inductor has a current switching ripple of 40 kHz.

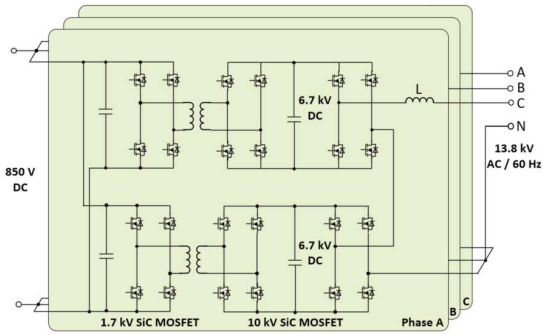

Fig. 1. PCS converter topology.

The AC side filter inductor is designed considering the grid requirements. The inductance is 44 mH (0.009 p.u.), which is mainly determined by the grid-side current harmonic requirement. The inductor needs to have an inrush current capability of 23 A, considering the grid transient. More converter parameters are shown in Table I.

TABLE I. CONVERTER PARAMETERS

Converter parameters	MV AC grid voltage	13.8 kV
	LV DC grid voltage	850 V
	Power rating	100 kW
	MV DC-link voltage	6.7 kV
	Switching frequency	10 kHz
Inductor parameters	Inductance	44 mH (0.009 p.u.)
	RMS current	4.2 A
	Inrush current	23 A
	Current ripple frequency	40 kHz
	Temperature rise	80 ºC
	Cooling	Natural air

The inductor was first designed without considering the insulation requirements. At first, a low window fill factor was assumed, and after the insulation has been designed, if the window fill factor does not meet the requirement, then another window fill factor will be used. Therefore, it needs some iteration to get the final design results. In this paper, the iteration is not discussed in detail, and only the final design results are introduced.

The amorphous core is selected as the inductor core considering its high saturation flux density (~ 1.5 T) and low core loss, considering the 40 kHz current switching ripple. The inductor basic design results are shown in Table II.

TABLE II. INDUCTOR BASIC DESIGN RESULTS

Core material	Amorphous
Core size	AMCC0500
Winding turns	330
Wire gauge	AWG 19
Air gap	5.0 mm
Core loss	18 W
Wire loss	44 W

III. INDUCTOR INSULATION DESIGN

According to IEC 60071-1 (2006) [9], the insulation requirements for equipment in the 13.8 kV grid are 95 kV for the rated lightning impulse withstand voltage and 31 kV root mean square (RMS) for the rated short-duration (1 minute) power frequency withstand voltage. Therefore, the inductor insulation design should refer to these requirements.

In this paper, the inductor is designed to be dry type with resin-encapsulated winding. The insulation within the winding itself and the insulation between the winding and the core (or ground) are separately discussed first.

A. Turn-to-turn and Layer-to-layer Insulation

The instantaneous voltage applied on the inductor during the converter operation equals the grid voltage minus the converter output PWM voltage.

In the normal operation, the maximum inductor voltage occurs when the grid voltage equals zero, and in this case, the inductor peak voltage is the same as the MV DC-link voltage, which is 6.7 kV.

The standard 31 kV RMS short-duration test is mainly used to test the reliability of equipment in the 13.8 kV system, considering the grid transients, such as switching transient, resonance, and transformer energizing. During the converter operation, an overvoltage could happen, and the voltage applied on the inductor winding is also higher than the normal operation. Therefore, assuming the 31 kV RMS short-duration test voltage is applied on the inductor can ensure the inductor insulation capability.

For a 13.8 kV system, the standard rated lightning impulse withstand voltage is 95 kV, which means all equipment connected to this system need to have a withstand voltage not lower than 95 kV [9]. Although arresters are installed, and they will clamp the lightning surge voltage at a certain level lower than 95 kV, some margin is essential to avoid insulation failure. Therefore, the winding insulation also considered the 95 kV.

Therefore, the inductor winding voltage stress is

$$v_{L\_max} = \begin{cases} 6.7\ kVpk & in\ normal\ operation \\ 44\ kV\text{pk} & short-duration \\ 95\ kVpk & lightning\ impulse \end{cases} \quad (1)$$

Based on the basic design, the inductor has 330 turns in total. The winding structure shown in Fig. 2 is mostly used in the LV transformer and inductor and is first considered in the inductor design. Considering the window area and wire gauge, the 330 turns are divided into 10 layers, with 33 turns in each layer, and each core leg has 5 layers. Although the turn-to-turn insulation requirement is the lowest, which is 1/330 of the inductor voltage stress, the layer-to-layer voltage stress is around 66/330 of the inductor withstand voltage. Assume the inductor voltage is evenly distributed among winding turns, then the layer-to-layer voltage will be 1.34 kV, 8.8 kV, and 19 kV during the normal operation, short-duration, and lightning transient, respectively. This requires thick insulation layers between winding layers. Therefore, this winding structure is not preferred for this inductor.

To reduce the layer-to-layer voltage stress, a winding

structure shown in Fig. 3 is designed. The 330 winding turns are divided into 22 sections (S1 to S22), with 15 turns in each section. With this structure, although the turn-to-turn voltage stress is increased from 1/330 to 6/330 of the inductor voltage, the layer-to-layer voltage stress is reduced from 66/330 to 25/330 of the inductor voltage. One advantage of the designed winding structure is that the section spacers can be integrated with the inductor bobbin, and they can be made with insulation material. Another advantage is that this structure contributes to the transient voltage distribution among the winding turns.

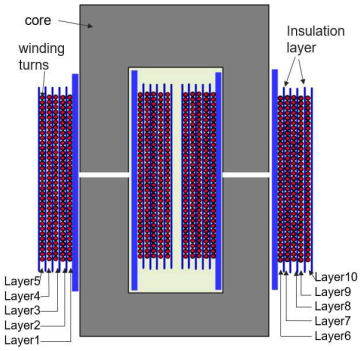

Fig. 2. Normally used inductor winding structure.

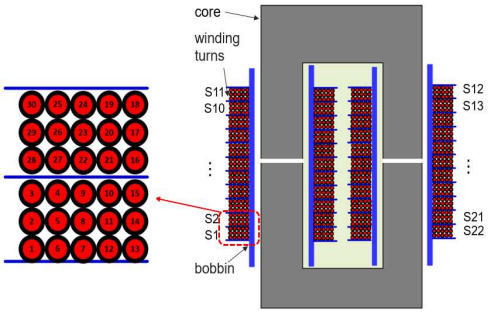

Fig. 3. Designed inductor winding structure.

The winding bobbin together with the section spacers is directly printed out with Formlab's high-temperature 3D printing material, which has a dielectric strength of 21.6 kV/mm. Considering the strength of the spacer and also the wire diameter, the section spacer thickness is determined at 1.4 mm.

The designed inductor bobbin is shown in Fig. 4, the windows cut on the bobbin are used to get the potting material flows into the gaps among wires. Also, 6 mm insulation spaces at the top and bottom sides are designed.

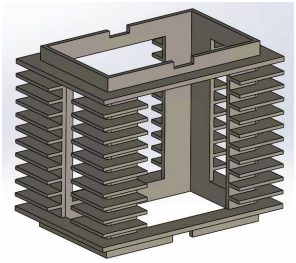

Fig. 4. Designed inductor bobbin.

B. *Winding-to-core/ground Insulation*

For safety consideration, the cores will be grounded. Then, the insulation requirements between the winding and the core are 31 kV RMS for short-duration and 95 kV for lightning. 50-3170 epoxy is selected as the potting material for its high thermal conductivity (1.73 W/m-K) and high dielectric strength (18.9 kV/mm). Based on the literature, the long-term electrical strength of epoxy is usually around 6 -10 kV/mm for given manufacturing technology [10]. In this design, 7 kV/mm is assumed for the normal operation and short-duration voltage withstand. For the lightning, since it is quite short in time, a time factor of 0.45 can be used when considering the insulation material capability, which means 15.6 kV/mm of insulation capability can be considered. Therefore, the insulation distance should be

$$d_{insulation} = \begin{cases} 4.43\ mm & for\ normal\ and\ short-duration \\ 6.09\ mm & for\ lightning \end{cases} \quad (2)$$

An inductor winding case is designed, as shown in Fig. 5, to contain the winding and ensure the insulation distances.

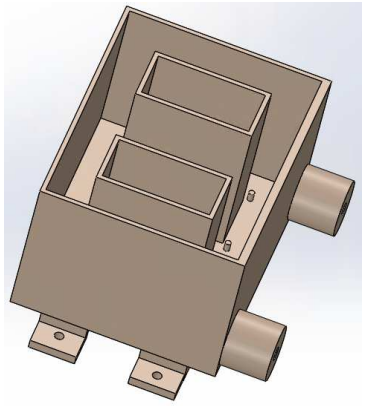

Fig. 5. Designed inductor winding case.

The assembly of the inductor winding case and two bobbins is shown in Fig. 6(a), and the assembly with the core is shown in Fig. 6(b).

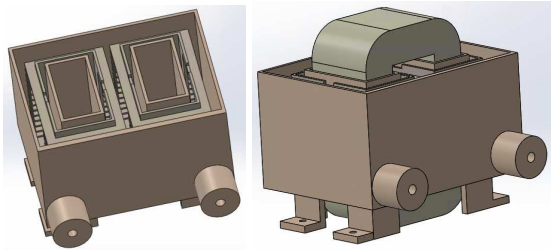

(a) (b)

Fig. 6. Assembly of (a) the winding case and two bobbins, and (b) the winding case, bobbins, and the core

The cross-sectional dimensions of the inductor case and bobbins are shown in Fig. 7. Both the winding case and the bobbins are 3D printed with the same material. Since it has a similar dielectric strength as the potting material, the thicknesses of the winding case and bobbins can also be treated as insulation distances. Therefore, the insulation distance between the winding and the inductor surface is around 9 mm, which is higher than the requirement shown in (2).

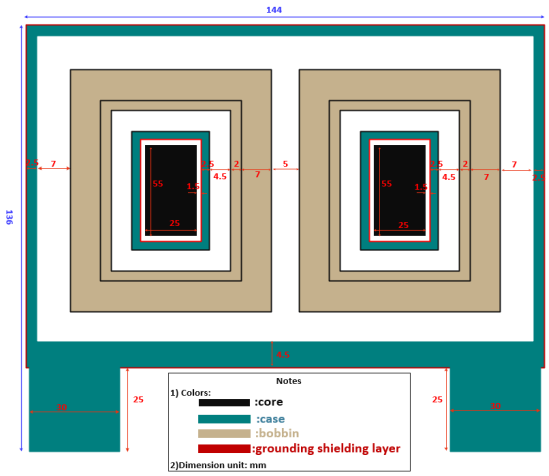

Fig. 7. Cross-sectional dimension of the inductor.

C. Grounding Shielding

The core and the inductor winding case cannot perfectly match with each other, and there would be air gaps between them, which may result in PD, especially during the lightning transient.

To avoid the discharge of these air gaps, the winding case surface is coated with a thin copper shielding, which is grounded together with the cores. This shielding layer gives a constant potential to the winding case surface, and the voltage between the inductor winding and ground is all stressed on the insulation material, i.e, the potting material and the 3D printing material.

Also, this shielding layer can act as a noise shielding, preventing the EMI noise of the inductor winding from going to the environment.

One drawback of this design is that the shielding layer increases the parasitic capacitance between the winding and the ground, which will increase the transient current spike flowing through the inductor and devices and then increase the overall converter losses.

D. Local Area Electric Field

Although with the shielding layer, the voltage stress is mainly distributed among the insulation materials, it is essential to check the local electric field to make sure that the maximum electric field does not exceed the material capability.

From the simulation on Ansys/Maxwell, it is found that the terminations are critical points in terms of the electric field. As shown in Fig. 8, the shielding layer ended at the winding terminal side. Based on the electric field simulation, the electric fields at the terminations of the shielding layer are higher than that of other places. Increasing the insulation distance can decrease the local electric field. Finally, the maximum local electric field is controlled to be below 7 kV/mm by adjusting wire terminal length and diameter.

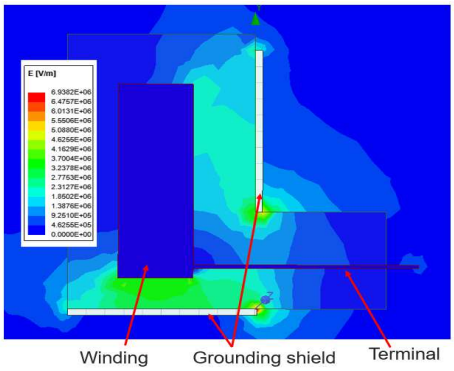

Fig. 8. Electrical field analysis.

IV. Inductor Building and Insulation Testing

A. The 1st Verison of Inductor

As shown in Fig. 9, the inductor windings are wound on two separate bobbins, which are 3D printed with high insulation material. The two magnetic wire terminals are led out with two high voltage cables rated at 42 kV DC.

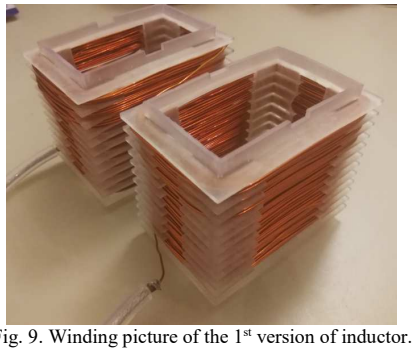

Fig. 9. Winding picture of the 1st version of inductor.

The designed inductor has been successfully built, as shown in Fig. 10. The overall dimension is 5.67" W × 5.41" H × 5.75" L, including the winding terminals.

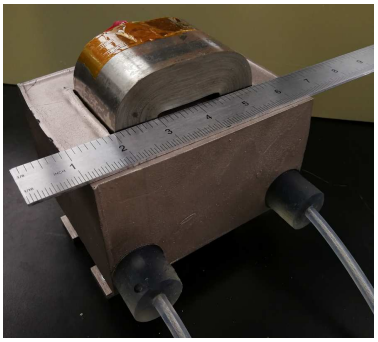

Fig. 10. Picture of the 1st version of inductor.

B. Insulation Test of the 1st Version of the Inductor

The DC hi-pot test was carried out with PHENIX 4100-10 hi-pot tester, and the hi-pot voltage was applied between the winding terminals and the shielding layer. The applied hi-pot test voltage was gradually increased from 0 to 48 kV, which is around the peak value of 31 kV RMS, and no breakdown had been observed during the testing process. The leakage current read from the hi-pot tester at some voltage

levels had been recorded, and at each voltage level, the testing had been conducted for more than one minute.

Fig. 11 shows the relationship between the applied voltages and the recorded leakage currents. It can be found that the leakage current linearly increases with the applied voltage, which means the insulation between the winding and the shielding layer is mainly high resistive and the impedance is around 4.3 GΩ.

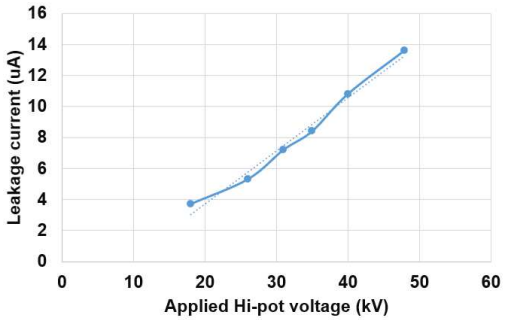

Fig. 11. Hi-pot test results of the 1st version of inductor.

The PD test was conducted, too. However, the PD inception voltage (PDIV) is around 3.8 kV RMS, which is much lower than the expected value. The main reasons for the low PDIV are

1) The epoxy used has a high viscosity, and the potting process used cannot remove all the air inside the epoxy, so there are some air bubbles in the winding.

2) As shown in Fig. 9, there are some soldering points for the wire connection. Some sharp soldering conductor could exist there and will lead to a high local electrical field, causing PD.

V. Operational Test

A. Preliminary Test

The inductor was first tested with a half-bridge of the PCS converter for insulation and thermal consideration. The test setup diagram is shown in Figure 12, and the switching frequency of the 10 kV SiC MOSFETs is 10 kHz. The applied DC-link voltage was gradually increased from 0 to 7 kV, and the modulation index was adjusted to get a rated current, i.e., 4.2 A RMS / 60 Hz.

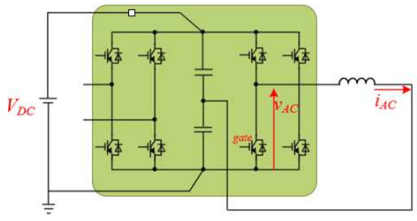

Fig. 12. Preliminary test setup diagram.

Waveforms of the gate driver signal of the lower device, the inductor current, and the switching node voltage are shown in Fig. 13. The inductor current has a lot of switching ripples because the PWM voltages are all applied to the inductor.

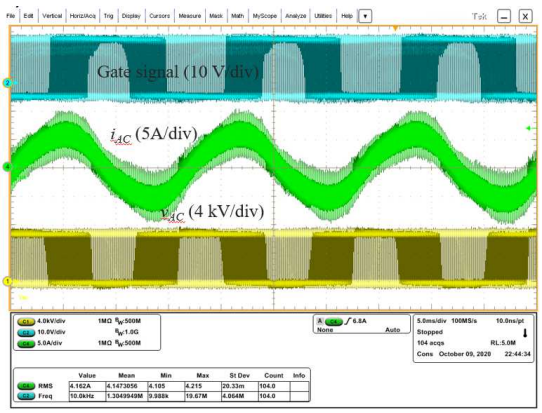

Fig. 13. Winding test waveforms.

The inductor temperature was measured with a thermal camera after it went to thermal equilibrium. As shown in Fig. 14, the room temperature is around 20 ºC, and the maximum temperature of the inductor is around 56 ºC, so the temperature rise is around 36 ºC.

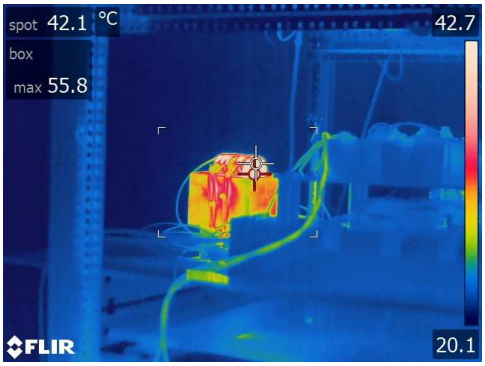

Fig.14. Inductor thermal image.

B. Single Phase Test

After the half-bridge test, the inductor was assembled into the single-phase PCS converter for further test. As shown in Fig. 15, an LV DC power supply was used to supply the single-phase converter from the LVDC side. The PCS MV AC side is connected to an MV transformer, of which the LV AC side is connected to a Variac. In this test, the insulation test was the focus, so no load was connected, and the PCS converter only supplies the magnetizing current of the MV transformer.

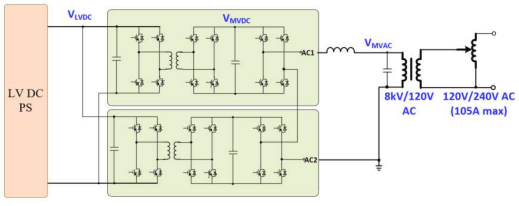

Fig.15. Single-phase test setup diagram.

The test was conducted up to 800 V at the LVDC side, which is corresponding to 6.3 kV at each MVDC bus and 7.5 kV RMS at the MVAC output. The waveforms of the MVAC voltage and inductor current are shown in Fig. 16.

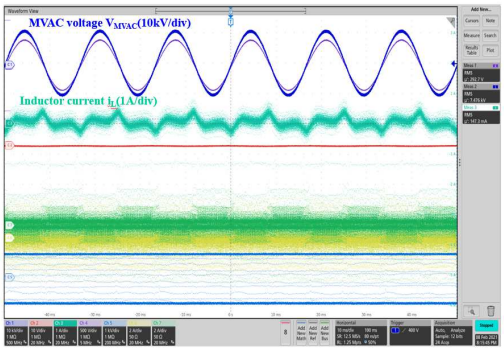

Fig.16. Single-phase test waveforms.

VI. Issue Found and the New Inductor

A. Overheat Issue

During the 7.5 kV RMS MVAC testing, an overheat issue had been found on the inductor. During the test, two thermal sensors were applied on the surface of the winding and core, respectively. The temperature number read from the core and winding sensors are 70 ºC and 110 ºC, respectively, of which the core temperature is as expected, but the winding temperature is much higher than expected. Since the load current was small, the copper loss was smaller than that in the rated case. Therefore, some other losses, which were not anticipated, occurred.

Fig. 17 shows the thermal image of the inductor, which was taken after the converter had been shut down for around 5 minutes, so the maximum temperature is lower than that during the test. However, the temperature distribution can still be observed from it, and it can be found that the space between the inductor upper core and winding was heated up.

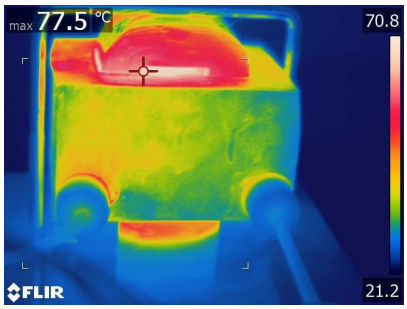

Fig.17. Inductor thermal image taken after test ended for 5 minutes.

The charge and discharge of the parasitic capacitance result in some extra losses, but these losses should not concentrate on a narrow space. Also, all the charge and discharge paths share the loss, so it should not be that much in the inductor winding itself.

Therefore, a highly possible reason is the PD. During the potting process, the air bubbles moved upward to the top side of the inductor winding; but did not break due to the high viscosity of epoxy. Then, during the test, PD happened around air bubbles, and a lot of heat generated at the top side of the winding. Besides, the space between the winding top surface and the core is narrow, so the heat could accumulate there. Because of the air gap, the heat cannot be effectively transferred to the core, so the core has a lower temperature than the winding, although they are close to each other.

B. Inductor Design Improvement

Based on the test results discussed above, the inductor design has been improved, and the main improvements are:

1) The two winding terminals are directly led out so that no soldering is needed.

2) Grading rings are added at the two terminations, to increase both the clearance and creepage distance at the winding terminations.

3) DOWSIL TC-4605 HIL thermally conductive encapsulant has been used as the potting material. Compared to the epoxy used in the 1st inductor, this material has a much lower viscosity, which will make it easier to de-air and reduce the air bubble in the winding.

C. The 2nd Version of the Inductor

The 2nd version of the inductor has been built, as shown in Fig. 18, and its dimension is 5.91” W × 5.41” H × 6.50” L, including the two winding terminals.

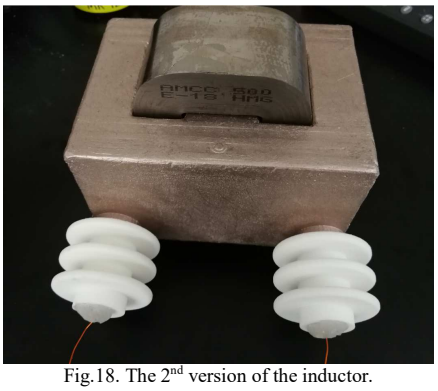
Fig.18. The 2nd version of the inductor.

D. Insulation Test for the 2nd Version of the Inductor

The DC hi-pot test was first conducted with the same tester and the same test process. The leakage currents at different hi-pot voltage levels are shown in Fig. 19. It can be found that in the tested voltage range, the leakage current kind of linearly increase with the voltage, and the insulation impedance is around 95 GΩ. Compared to the 1st version of the inductor, the insulation impedance of the new inductor has been increased more than 20 times.

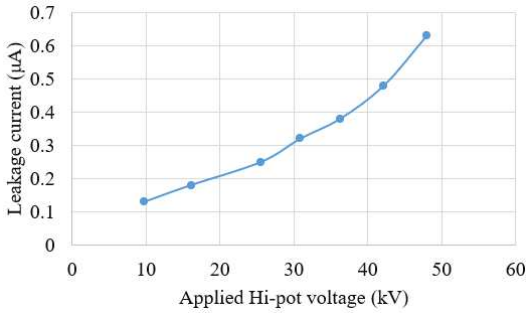

Fig.19. Hi-pot test results of the 2nd version of the inductor.

Then, the PD test was conducted. As shown in Fig. 20 and Fig. 21, the PDIV is around 8.8 kV RMS and the inductor

passed the PD test up to 12.1 kV RMS (<50 pC). The PD performance of the new inductor is improved more than 2 times, compared to that of the 1st version of the inductor. This PDIV is already sufficient for the PCS converter operation voltage, which is 8 kV RMS.

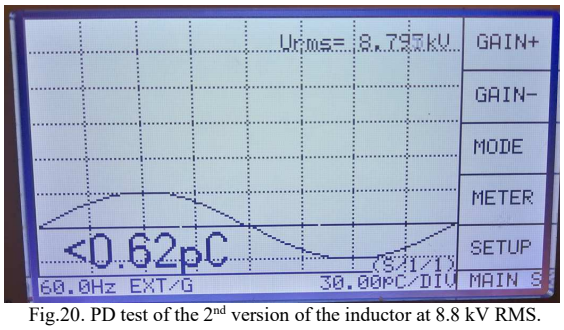

Fig.20. PD test of the 2nd version of the inductor at 8.8 kV RMS.

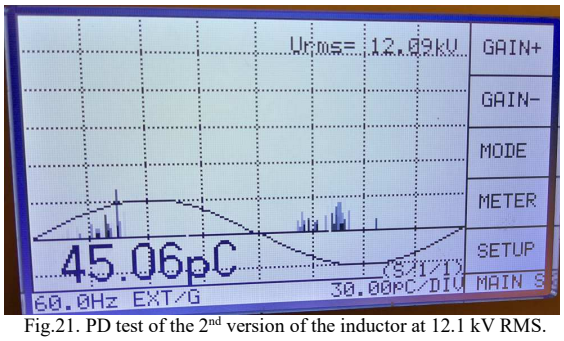

Fig.21. PD test of the 2nd version of the inductor at 12.1 kV RMS.

VII. Conclusion

This paper has discussed the insulation design of the filter inductor in a 13.8 kV grid-connected PCS converter. The inductor insulation design considered the short-duration (1 minute) power frequency withstand voltage and lightning impulse voltage required in IEC 60071-1 (2006). Winding bobbins were designed to reduce the voltage stress between adjacent layers/sections, and a winding case was used to contain the bobbins and ensure the insulation distance between windings and core/ground.

Based on the design, the 1st version of inductor was built and first tested with DC hi-pot test and PD test. Then, the inductor was tested in the single-phase PCS converter, operated at 7.5 kV RMS. However, overheat issue was found on the 1st version of the inductor during the 7.5 kV RMS single-phase test.

To address the overheat issue and improve the PD performance, the inductor design was improved, and a 2nd version of the inductor was built. Compared to the first inductor, the insulation impedance of the new inductor is improved more than 20 times, and the PD test result of the new inductor is increased more than 2 times. The new inductor will be further tested in the single-phase PCS converter.

Acknowledgment

This work was supported primarily by the Advanced Manufacturing Office (AMO), United States Department of Energy, under Award no. DE-EE0008410. This work made use of the shared facilities of the Engineering Research Centre Program of the National Science Foundation and the Department of Energy under NSF Award no. EEC-1041877. The authors would like to acknowledge the contribution of Southern Company and Powerex.

References

[1] J. Thoma, B. Volzer, D. Kranzer, D. Derix, and A. Hensel, "Design and Commissioning of a 10 kV Three-Phase Transformerless Inverter with 15 kV Silicon Carbide MOSFETs," in *20th European Conference on Power Electronics* and Applications (EPE'18 ECCE Europe), 2018, pp. P.1-P.7.

[2] A. Anurag, S. Acharya, Y. Prabowo, V. Jakka and S. Bhattacharya, "Design of a Medium Voltage Mobile Utilities Support Equipment based Solid State Transformer (MUSE-SST) with 10 kV SiC MOSFETs for Grid Interconnection," *9th IEEE International Symposium on Power Electronics for Distributed Generation Systems (PEDG)*, Charlotte, NC, 2018, pp. 1-8.

[3] S. Madhusoodhanan *et al.*, "Solid-State Transformer and MV Grid Tie Applications Enabled by 15 kV SiC IGBTs and 10 kV SiC MOSFETs Based Multilevel Converters," *IEEE Transactions on Industry Applications,* vol. 51, no. 4, pp. 3343-3360, 2015.

[4] H. Zhao *et al.*, "Physics-Based Modeling of Parasitic Capacitance in Medium-Voltage Filter Inductors," *IEEE Transactions on Power Electronics,* vol. 36, no. 1, pp. 829-843, 2021.

[5] D. Rothmund, T. Guillod, D. Bortis, and J. W. Kolar, "99% Efficient 10 kV SiC-Based 7 kV/400 V DC Transformer for Future Data Centers," *IEEE Journal of Emerging and Selected Topics in Power Electronics,* vol. 7, no. 2, pp. 753-767, 2019.

[6] M. Kaymak, R. W. D. Doncker, and T. Jimichi, "Design and Verification of a Medium-Frequency Transformer in a Three-Phase Dual-Active Bridge DC-DC Converter for Medium-Voltage Grid Connection of Offshore Wind Farms," in *IEEE Applied Power Electronics Conference and Exposition (APEC)*, 2020, pp. 2694-2701.

[7] D. Dong, M. Agamy, J. Z. Bebic, Q. Chen, and G. Mandrusiak, "A Modular SiC High-Frequency Solid-State Transformer for Medium-Voltage Applications: Design, Implementation, and Testing," *IEEE Journal of Emerging and Selected Topics in Power Electronics,* vol. 7, no. 2, pp. 768-778, 2019.

[8] T. B. Gradinger, U. Drofenik, and S. Alvarez, "Novel insulation concept for an MV dry-cast medium-frequency transformer," in *19th European Conference on Power Electronics and Applications (EPE'17 ECCE Europe)*, 2017, pp. P.1-P.10.

[9] Insulation co-ordination – Part 1: Definations, principles and rules. IEC 60071-1, 2006.

[10] E. Ostapenko, V. Trifonov, V. Varivodov, "long-term dielectric strength of cast epoxy and composite insulators," *CIGRE*, 2004.